



Synthesis Optimization of Piezo Driven Four Bar Mechanism Using Genetic Algorithm

Laith Sawaqed¹, Khaled S. Hatamleh^{1,2}, Mohammad A. Jaradat^{1,2},
Qais Khasawneh^{1,3}

¹Mechanical Engineering Department, Jordan University of Science & Technology, P.O.Box 3030 Irbid, Jordan
kshh@just.edu.jo, majaradat@just.edu.jo, gakhasawneh@just.edu.jo

²Mechanical Engineering Department, American University of Sharjah, P.O. Box (2666) Sharjah, UAE
khatamleh@aus.edu, mjaradat@aus.edu

³Electromechanical Engineering technology department, Institute of Applied Technology, Abu-Dhabi, UAE
Qais.khasawneh@adpoly.ac.ae

ABSTRACT

Over the past few years, there has been a growing demand to develop efficient precision mechanisms for fine moving applications. Therefore, several piezoelectric driven mechanisms have been proposed for such applications. In this work an optimal synthesis of a four-bar mechanism with three PEAs is proposed. Two evolutionary multi-objective Genetic Algorithms (GAs) are formulated and applied; A Genetic Algorithm Synthesis method (GAS) is first used to obtain a synthesis solution for the mechanism regardless of power consumption. Then another Genetic Algorithm Minimum Power Synthesis method (GAMPS) is used to obtain the synthesis solution of minimum power consumption. For that purpose, the study performs simulation investigation of the aforementioned algorithms for each point along sinusoidal and kidney shaped paths of motion. Results show capability of both methods in obtaining a synthesis solution. However, GAMPS outperformed GAS in terms of driving power consumption as it is minimized by 99% ratio.

KEY WORDS: Genetic Algorithm, Four-bar Mechanism, Synthesis optimization.

1 INTRODUCTION

PIEZOELECTRIC actuators (PEAs) provide micro-level fine tuning and precise positioning control. Therefore, PEAs were deployed within several mechatronic system applications that require such positioning accuracy over the last decade. For instance, PEAs were proposed to run hard disk drives and micro-manipulator mechanisms (Nambi, et. al. (2012); Lopez-Martinez and Campo (2003); Krishnan and Saggere (2007); Tan (2001); Liaw, et. al. (2008); Liaw and Shirinzadeh (2009); Lin and Lin (2012)). However, the proposed solutions consist mainly of multi bar mechanisms with coupled links. This in turn, created a challenge in obtaining a valid and optimum synthesis solution.

Zhang, et. al. (1984) presented an atlas of curves that approximates the geometrical solution needed to follow a desired path by a geared five-bar mechanism; each of those curves is associated with a certain gear

phase angle. However, the approximated solutions need an optimization process for accurate path following.

Chanekar and Ghosal (2013) introduced a two-stage sequential quadratic based optimization algorithm for synthesis of adjustable planar four-bar mechanisms to solve a continuous path generation problem. The first stage of the algorithm obtains possible driving dyads, which are then passed on to the second stage to obtain the remaining mechanism parameters using least-squares based circle-fitting procedure. The authors used an objective function that is based on the geometry of the four bar mechanism. Synthesis results presented by two numerical examples using the proposed method demonstrated more efficient optimization than literature work as it uses less number of design variables in the search process.

Gogate and Matekar (2012) presented two evolutionary new objective functions for optimum synthesis of mechanisms path generating. The authors used Differential Evolution optimization to assess the performance of the presented new objective functions through several simulations runs over a four-bar mechanism three different prescribed paths of motion. Obtained Results are compared with those generated using the regular tracking error function between followed path and desired path. The presented objective functions are concluded as better option for optimization in accordance to designer interest and problem nature.

Recently, simplicity of implementation and fast convergence speed realized by powerful computers encouraged other researchers to use modern optimization and evolutionary techniques to solve complex mechanisms synthesis such as Diab and Smaili (2017); Yi and Liu (2017). For instance, Cabrera, et. al. (2002) used simulation techniques to achieve minimal error between the desired and actual paths of motion followed by planner mechanism using Genetic Algorithms (GA). Another study presented by Laribi, et. al. (2004) in which a fuzzy logic is proposed to adjust the initial bounding intervals used by GA for path generation of a four-bar mechanism synthesis, simulation results of the Fuzzy GA method against classical GA method show higher accuracy and faster convergence. Cabrera, et. al. (2007) applied an evolutionary GA based technique "POEMA" to optimize a multi-objective synthesis problem of a planar hand robot. The study extended "POEMA" using Pareto-based approach to classify the outcomes and choose the optimal solution. The fast convergence results were encouraging to be used for other mechanism synthesis. Affi, et. al. (2007) considered both mechanism synthesis and motor characteristics while controlling a motor-driven four-bar system using multi-objective optimization approach. Continual efforts in the field, were carried out such as; the work done by Acharyya and Mandal (2009), in which a synthesis of a four-bar mechanism for trajectory following was done using GA, Particle Swarm Optimization Technique (PSO), and Differential Evolution (DE). The latter outperformed GA and PSO. In 2009, Erkaya and Uzmay (2009) were able to minimize deviations of a four-bar mechanism from desired path of motion arising from clearance; where two GA were used to minimize trajectory errors after obtaining direction of joint clearance using minor search space knowledge. Khorshidi, et. al. (2011) presented a multi-objective optimization algorithm for path-generation of four-bar linkage mechanisms. The proposed algorithm used Pareto Genetic algorithm to enhance the performance of a Non-dominant strong Genetic algorithm by setting the radius of the local search neighbourhood at each search step. The presented hybrid algorithm used triple-objective functions at once during optimization

namely; minimum tracking error, deviation from 90 degrees angle in addition to maximum angle velocity ratio. Optimization results using the proposed algorithm over four-bar mechanism's path generation design outperformed other literature algorithms in terms of energy efficiency, computational power, and practical viability.

Recently, El-kribi, et. al. (2013) used Non-dominant Strong Genetic Algorithm to select the optimal motor and optimal inertia distribution of a considered motor driven mechanical system. The proposed algorithm used minimum motor torque and minimum velocity fluctuation as objective functions. Obtained results of the optimal (driving motor/mechanical system properties) proved to be more efficient than electromechanical design strategies. In addition, the algorithm was able to minimize considered system power consumption and velocity fluctuation without the need of sophisticated controllers.

However, the majority of the discussed solutions within the literature did not include the type of driving system for the proposed solution. Although PEAs were deployed within fine tuning applications for high precision mechanisms, they suffer from the nonlinear behaviour that affects motion accuracy and makes it more challenging to find their synthesis solution (Liaw, et. al. (2008); Liaw and Shirinzadeh (2009); Lin and Lin (2012)).

In this paper, unlike the conventional four bar mechanism (Oetomo, et. al. (2006); Sitti (2003); Tari and Su (2011)), due to the lack of a closed form solution for the inverse kinematics of the piezo-driven four bar mechanism with 6 variables, a multi-objective optimization of the mechanical system using PEAs is presented, namely, the four-bar mechanism, as illustrated schematically by Figure 1. Optimal synthesis is achieved based on a genetic algorithm approach. The objective functions are used to minimize both the deviation of the end effector location from the desired position, and the change in the four-bar mechanism links lengths which guarantee reduced power consumption of the PEAs when it moves from one position to another. Figure 1 shows a flexure-based four-bar mechanism driven by three PEAs. Accordingly, the main contribution is to determine the optimal inverse kinematic solution for the piezoelectric actuated four-bar mechanism to move the end effector to a predefined position by using genetic algorithm. The dynamical model of the deployed PEA in the mechanism is assumed to be compensated as in Lin and Yang (2006); Badr and Ali (2010).

The paper will be structured as follows: in Section 2, formulates the analytical model of the four bar mechanism. Section 3 states the dynamic model of the PEA. Section 4 formulates the optimization problem of the considered four bar mechanism. Section 5 illustrates the working principle of the genetic

algorithm and formulates the fitness function. Section 6 shows discussion of the simulation results based on defined fitness function. Finally, Section 7 summarizes the conclusions of this study.

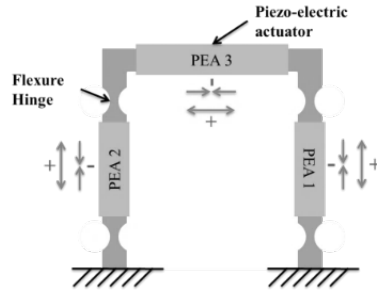


Figure 1: Piezo-driven flexure-based four-bar micro/nano manipulator.

2 MECHANISM MODELING

THE main objective is to provide an inverse kinematic solution for the piezoelectric actuated four-bar mechanism using GA. The mechanism end effector follows a desired path within its reachable workspace while considering the geometrical constraints of the mechanism. For this purpose, the four-bar mechanism shown in Figure 1 can be simplified into four links pinned together as shown in Figure 2. The dimensional synthesis model, as shown in KHALAF (2012), can be summarized as follows:

$$\begin{aligned} \|\vec{R}\| &= \sqrt{X^2 + Y^2} \\ X &= L + (L + \Delta L_1) \cos(\theta_1) \\ Y &= (L + \Delta L_1) \sin(\theta_1) \end{aligned} \quad (1)$$

When the mechanism's end effector is following some desired path, the deformation of the first piezoelectric (PEA1) link (ΔL_1) and its corresponding angular deflection (θ_1) are determined geometrically using Eqs. (2-3):

$$\Delta L_1 = \sqrt{(X - L)^2 + Y^2} - L \quad (2)$$

$$\theta_1 = \tan^{-1} \left(\frac{Y}{X - L} \right) \quad (3)$$

where L is the original link length, (X, Y) are coordinates of the desired end effector location, and θ_1 is the orientation of the first link as shown in Figure 2.

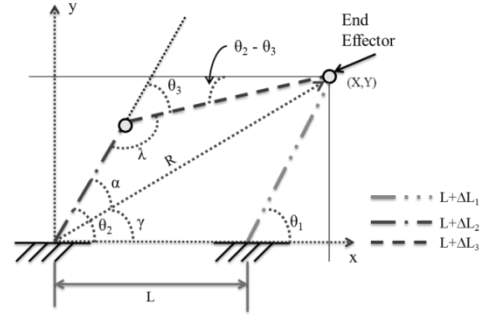


Figure 2: Simplified four-bar mechanism.

Since the first link has a unique solution, then the synthesis problem is reduced into solving for the deformations of the second and third (PEA2 & PEA3) links which are referred to as ($\Delta L_2, \Delta L_3$) and their corresponding angular deformations (θ_2 & θ_3). Based on geometry and parameters shown in Figure 2, the following relations can be determined as:

$$\gamma = \tan^{-1} \left(\frac{Y}{X} \right) \quad (4)$$

$$\begin{aligned} \theta_2 &= \alpha \pm \gamma \\ \alpha &= \begin{cases} \theta_2 - \gamma & , \theta_2 \geq \gamma \\ \gamma - \theta_2 & , \theta_2 < \gamma \end{cases} \end{aligned} \quad (5)$$

$$c\lambda = \frac{(L + \Delta L_2)^2 + (L + \Delta L_3)^2 - (x^2 + y^2)}{2(L + \Delta L_2)(L + \Delta L_3)} \quad (6)$$

$$\sin \lambda = \left(\frac{\sqrt{X^2 + Y^2}}{(L + \Delta L_3)} \right) \sin \alpha \quad (7)$$

$$\lambda = \tan^{-1} \left(\frac{\sin \lambda}{\cos \lambda} \right) \quad (8)$$

$$\theta_3 = \begin{cases} +(180 - |\lambda|) & , \theta_2 < \gamma \\ -(180 - |\lambda|) & , \theta_2 > \gamma \end{cases} \quad (9)$$

The previous relations are coupled and hard to be solved individually for each parameter. However, they could be solved for an arbitrary numerical solution as introduced by Khalaf (2012), or by enumerative search methods, or by a soft computing methods such as GAs. In this paper, a multi-objective GA is used to solve for the optimal power unknown parameters $\Delta L_2, \Delta L_3, \theta_2,$ and $\theta_3,$ as shown in Figure 3, Where ζ_d is the desired end effector location represented by (x_d, y_d) coordinates

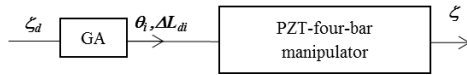


Figure 3: General block diagram for the proposed approach.

3 MODELLING

THE general model describing positioning mechanism using PEA is represented by mass spring damper system with an applied force from the PEA as presented in Lin and Yang (2006); Badr and Ali (2010). The general model developed by Bouc-Wen for the PEA describes the nonlinearity of the system by Lin and Yang (2006):

$$\begin{aligned} m\ddot{l} + b\dot{l} + kl &= f = k(du - h) + \rho \\ \dot{h} &= \alpha\dot{v} - \beta|\dot{v}|h - \gamma\dot{v}|h| \end{aligned} \quad (10)$$

where m represents the effective mass of the PEA, b is the damping coefficient, k is the stiffness, f the generated force due to the applied voltage to the PEA, d represents the ratio between the output displacement and applied input voltage u to the actuator, h represents the hysteretic nonlinear term for the PEA, l is the output displacement of the piezoelectric actuated mechanism in its respective dimension, $\rho = kl_0$ and l_0 is the initial displacement of the actuator as the applied voltage is $u=0$; α, β, γ are the parameters which characterizes the hysteretic loop's magnitude and shape of the PEA actuator. Finally \dot{l}, \dot{h} and \dot{h} are the derivatives of l and h with respect to time t , respectively. The modelling parameters using the Bouc-wen model were determined in Lin and Yang (2006).

The modeled hysteresis of the PEA is compensated by a feedforward loop for fine tuning application which mainly focuses on the motion manipulation, based on this approach the system is represented by Lin and Yang (2006) as:

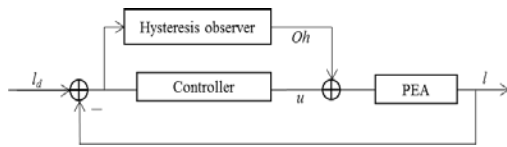


Figure 4: PEA feedforward compensator loop (Lin and Yang (2006)).

The controller command is the summation from the feedforward controller output $u(t)$ and the hysteresis observer output $oh(t)$ given as in equation (2)

$$U(t) = u(t) + Oh(t) \quad (11)$$

While the augmented closed loop model of the system is given as Lin and Yang (2006)

$$\dot{X} = AX + Bl_d \quad (12)$$

where $x_1=l$, $x_2 = \dot{x}_1$ and $x_3 = e(t) = l_d - l(t)$. For position fine tuning application a proportional integral (PI) controller was proposed by Lin and Yang (2006) to handle the system hysteresis based on linear matrix inequality approach. Where the augmented closed loop model of the system matrices are given as

$$A = \begin{bmatrix} 0 & 1 & 0 \\ K_c & B_c & 0 \\ -1 & 0 & 0 \end{bmatrix}, \quad B = \begin{bmatrix} 0 \\ u_c \\ 1 \end{bmatrix} \quad (13)$$

where B_c and K_c are the closed loop augmented damping coefficient, and stiffness, respectively.

$$u_c = \frac{d \times k \times k_p}{m} \quad (14)$$

where k_p is the controller proportional term.

4 OPTIMIZATION

TWO scenarios will be considered. The first compromises optimization of the four bar mechanism geometrical synthesis, while the second compromises optimization of the four bar mechanism geometrical synthesis along with minimum change in the four-bar mechanism links length which guarantee reduced power consumption. The optimization problem can be formulated as follows (El-kribi, et. al. (2013)):

$$\min : \quad g_j(Z), \quad j=1, \dots, n \quad (15)$$

$$\text{subject to :} \quad z_i \in [z_{i_{\min}}, z_{i_{\max}}]; \quad z_i \in Z \quad (16)$$

where g_j is the objective function. Z is a design vector of the four-bar mechanism, which contains all the design variables. $z_{i_{\min}}$ and $z_{i_{\max}}$ define the limits of each design variable z_i .

Consider the mono-objective function

$$g = \sum_{j=1}^n \mu_j g_j(Z) \quad (17)$$

where μ_j 's are arbitrary weighting factors, g_j ($j=1, \dots, n$) are the objective functions to be optimize. The weighting factors can be chosen based on the importance of the objective to the system for a given the application.

5 GENETIC ALGORITHM

GA is a soft computing method that can efficiently determine global minima/maxima of linear or nonlinear problems. GA is highly recommended for problems involving large number of unknowns that are hard to be determined using conventional methods. It is mainly based on the natural selective principle in which the fittest candidates in a population are selected as parents from which a replacement population is generated by mutation and crossover

operations to create better fit candidates often called offsprings (Haupt and Haupt (2003); Holland (1992)).

Figure 5 shows flow of the suggested GA until the stopping criteria is reached, i.e. maximum number of iterations (epochs) is reached or fitness values dropped below a predefined certain threshold. Generally the GA started with generating an initial population which consists of N random chromosomes. The algorithm optimizes a design variables vector Z (Chromosome) that contains the four unknown parameters (Genes):

$$Z = [\Delta L_2 \ \Delta L_3 \ \theta_2 \ \theta_3] \quad (18)$$

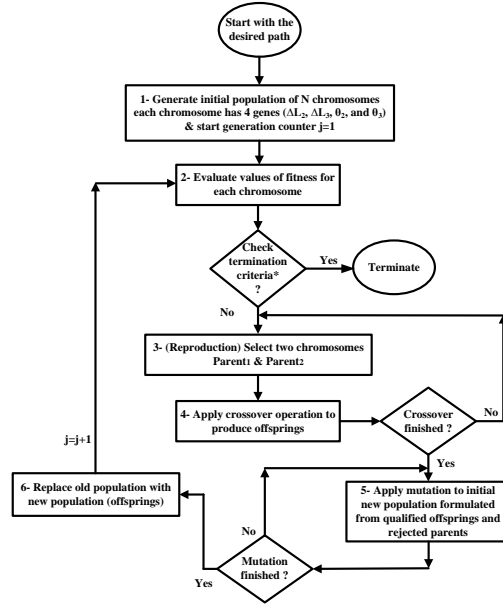


Figure 5: Genetic Algorithm block diagram (Hatamleh et al. 2015).

Next a fitness function is utilized to rank the proposed N random chromosomes. The best among the proposed is selected and passed to next generation; the size of the population is maintained by replacing the non-selected chromosomes by replacement process to create offsprings by mutation and crossover operations based on the selected chromosomes. Then the process is repeated until the best fit solution is achieved or the maximum number of generation is reached (* in Figure 5). In this paper two fitness functions are considered.

5.1 Genetic Algorithm Synthesis (GAS)

The fitness function considered in this section is the squared error between the desired end effector position and the obtained end effector position based on mechanism geometry shown in Figure 2. Mathematically, it can be defined as:

$$g = e^2 = (x_d - x)^2 + (y_d - y)^2$$

$$x = (L + \Delta L_2) \cos(\theta_2) + (L + \Delta L_3) \cos(\theta_2 - \theta_3) \quad (19)$$

$$y = (L + \Delta L_2) \sin(\theta_2) + (L + \Delta L_3) \sin(\theta_2 - \theta_3)$$

where the desired end effector location is represented by (x_d, y_d) coordinates, and the end effector position, obtained from the geometry, is represented by $[(L + \Delta L_2) \cos(\theta_2) + (L + \Delta L_3) \cos(\theta_2 - \theta_3), (L + \Delta L_2) \sin(\theta_2) + (L + \Delta L_3) \sin(\theta_2 - \theta_3)]$. $\Delta L_2, \Delta L_3$ are the next required PEA deformations of links 2 and 3. Finally, (θ_2, θ_3) are the next angular positions of links 2 and 3, as shown in Figure 2. This objective function will be minimized to obtain the design variables defined in (14).

5.2 Genetic Algorithm Minimum Power Synthesis (GAMPS)

Here, the fitness function takes into consideration the fitness function defined in the previous section and the power consumption represented as the difference in PEA deformation when moving the end effector from the current to the following position, mathematically:

$$g = e^2 = (x_d - x)^2 + (y_d - y)^2 + \nabla \Delta L_2^2 + \nabla \Delta L_3^2$$

$$x = (L + \Delta L_2) \cos(\theta_2) + (L + \Delta L_3) \cos(\theta_2 - \theta_3) \quad (20)$$

$$y = (L + \Delta L_2) \sin(\theta_2) + (L + \Delta L_3) \sin(\theta_2 - \theta_3)$$

$$\nabla \Delta L_2 = \Delta L_2 - \Delta L_{2,j-1}$$

$$\nabla \Delta L_3 = \Delta L_3 - \Delta L_{3,j-1}$$

where, $(\Delta L_{2,j-1}, \Delta L_{3,j-1})$ are the current PEA deformations of links 2 and 3, and $(\theta_{2,j-1}, \theta_{3,j-1})$ are the current angular positions of links 2 and 3. Similar to the previous section, the objective function will be minimized to obtain the design variables defined in (18) based on not only the geometry error but also the power consumption. Based on the optimization defined above, equal weighting factors are considered. Table 1 summaries the genetic algorithm options value used in the conducted simulations.

Table 2 summaries the upper and lower bounds used to search for the optimal parameters.

Table 1: GA options value.

GA option	Value
Population size	50
Crossover fraction	80 %
Elite count	1
Mutation Rate	1%
Number of Generations	400

Table 2: The lower and upper bounds of the unknown parameters.

	ΔL_2 (μm)	ΔL_3 (μm)	θ_2 (radian)	θ_3 (radian)
Lower Bound	-30	-30	0	0
Upper Bound	30	30	π	π

6 RESULTS

SINCE the proposed micro-manipulator is required to manipulate micro-objects or particles along any arbitrary path, two simulation runs were conducted to obtain the mechanism's minimum power synthesis solution using developed GA. The runs used sinusoidal and kidney-shaped paths of motion. At each run the path was discretized into a series of consecutive points that starts from the mechanism's unactuated position and ends at the considered path end. There are infinite synthesis solutions for $Z = \{\Delta L_2, \Delta L_3, \theta_2, \text{ and } \theta_3\}$ when moving from a current point to the next point along the path of motion, the proposed GAS searches for an arbitrary synthesis solution using the objective function described by equation (19). On the other hand, GAMPS uses the objective function described by equation (20) to extract the synthesis solution that represents the minimized power consumption.

Obtained changes in length of PEA link 1 along all path points are obtained using equation (2). Links 2 and 3 on the other hand, has many possible solutions. Therefore, GAS and GAMPS will differ unless they coincide by chance. Figure 9 and 10 show obtained changes in lengths of PEA links 2 and 3, namely ($\Delta L_2, \Delta L_3$) along all points of defined path. As expected, the figures show how GAS solution has higher values of ($\Delta L_2, \Delta L_3$) than those obtained by the GAMPS solution. Figures also show the expected fluctuation in obtained changes of PEA lengths while moving from one point to another using the GAS solution. The GAMPS solution resulted in a smooth mechanism motion along the defined path, unlike the GAS solution which requires higher power rates with rough mechanism motion.

The *difference* vector between current and next PEA links length is calculated and recorded for all points of motion path as described by the following equation:

$$\nabla(\Delta L_m) = \Delta L_{m_j} - \Delta L_{m_{j-1}}, m = 1, 2, 3 \quad (21)$$

This equation is considered twice, once using the GAS solution, and another using the GAMPS solution. The net change in length of PEA link 1 [$\nabla(\Delta L_1)$], is the actual change required in PEA link 1 when the mechanism moves from one point to another. Differences of change in links 2 and 3 are shown in Figure 11 and 12, respectively. It can be clearly noticed that there is a great enhancement over the required difference in links lengths. $\nabla(\Delta L_2)$ and $\nabla(\Delta L_3)$ when GAMPS is used. Summations of all

difference values along the defined path of motion for PEA links 2 and 3 are illustrated in Table 3. The table shows how the total amount of absolute values of differences, closely related to the required power, are dramatically smaller for both kidney-shape and sinusoidal paths.

Table 3: Total sum of change in length of PEA links for GAS and GAMPS along kidney-shaped and sinusoidal paths.

Sum of absolute changes in (μm)	Kidney-Shape Path		Sinusoidal path	
	GAS	GAMPS	GAS	GAMPS
$\sum_{q=1}^r \nabla(\Delta L_2)$	296	0	358	0
$\sum_{q=1}^r \nabla(\Delta L_3)$	256	0	460	0

Figure 8 shows that the fitness value and the average distance between individuals (chromosomes) decrease with the number of iterations represented by the number of generations (50 generations is shown) which indicates the conversion to a solution of the optimal mechanism synthesis. Figure 6 shows four positions of the proposed mechanism along the kidney-shaped path of motion; at each position GAS and GAMPS solutions are indicated, if GAS solution is traced from position 1 to 4, it is clear how the mechanism behaves in a fluctuating type of motion. On the other hand, tracing GAMPS solution over the same figure reveals the smooth type of motion obtained. Path tracking animations are provided for kidney-shaped and sinusoidal paths. The previous discussion for kidney-shaped path is also verified by sinusoidal path as shown by Figure 7.

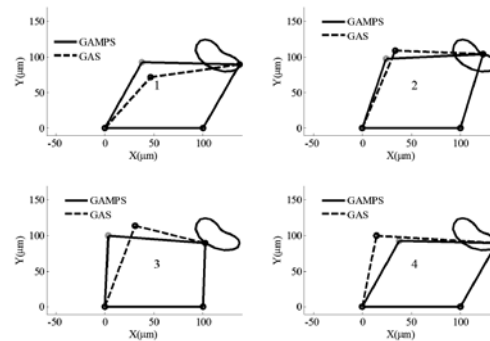


Figure 6: GAMPS vs. GAS solution snapshots along the kidney-shape path of motion.

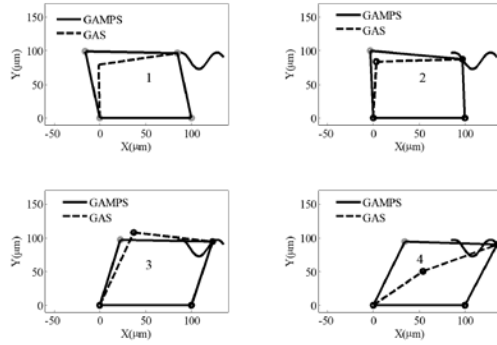


Figure 7: GAMPs vs. GAS solution snapshots along the sinusoidal path of motion.

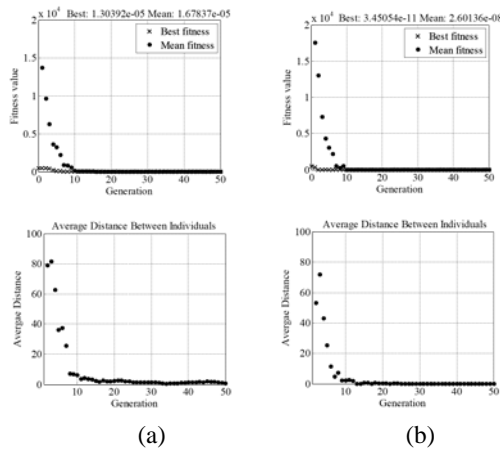


Figure 8: Fitness value and average distance vs. number of generations using (a) GAMPs, (b) GAS.

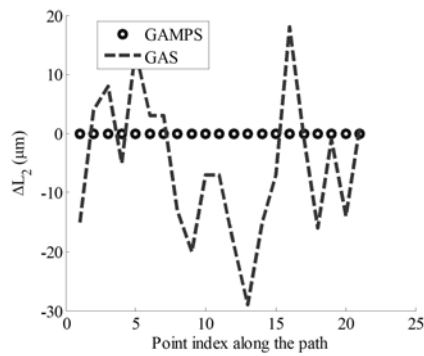


Figure 9: Deformation of PEA2 for kidney-shaped path.

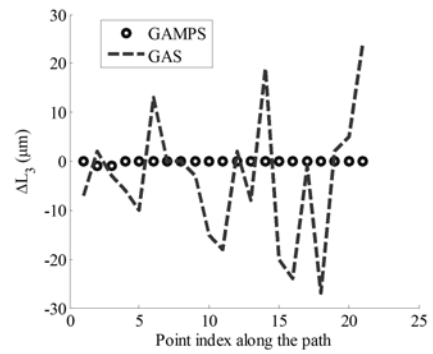


Figure 10: Deformation of PEA3 for kidney-shaped path.

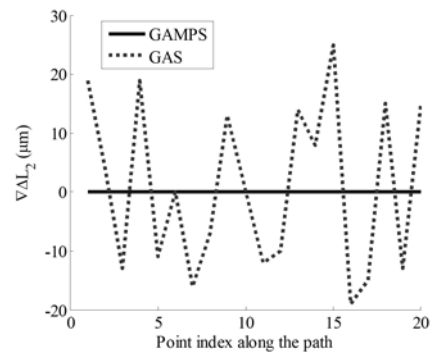


Figure 11: Required gradient in the second link deformation along the kidney-shape path.

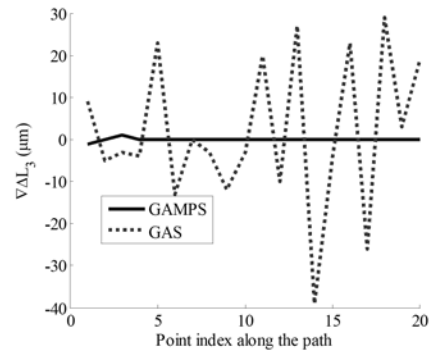


Figure 12: Required gradient in the third link deformation along the kidney-shape path.

7 CONCLUSION

AN optimal synthesis of a four-bar mechanism with three PEAs is proposed. The proposed mechanism synthesis for each point along the discretized path is a complex and computationally expensive process if conventional numerical and enumerative methods are used. In addition, these methods will result in multiple solutions that need optimization. Hence, Genetic Algorithm was proposed to obtain a synthesis solution at lower cost and faster

convergence. In order to achieve that, GAS and GAMPS were proposed to obtain a general synthesis solution and a minimum power synthesis solution, respectively. Simulation results tested over two different paths showed that GAMPS was able to obtain a solution that has less power consumption than GAS. Furthermore, it was noticed that the transition of mechanism links along the path were much smoother and had fewer fluctuations than GAS. The proposed GA can replace conventional numerical methods to synthesize other forms of multi bar mechanisms as it is easy to implement and has a faster convergence. Such advantages will make this approach more attractive to be deployed within feedback system to provide the required synthesis for the predefined path or set point.

8 REFERENCES

- S.K. Acharyya and M. Mandal, 2009. Performance of EAs for four-bar linkage synthesis. *Mechanism and Machine Theory*, 44(9), pp.1784–1794.
- Z. Affi, B. EL-Kribi, and L. Romdhane, 2007. Advanced mechatronic design using a multi-objective genetic algorithm optimization of a motor-driven four-bar system. *Mechatronics*, 17(9), pp.489–500.
- B.M. Badr and W.G. Ali, 2010. Nanopositioning Fuzzy Control for Piezoelectric Actuators. *International Journal of Engineering & Technology*, 10(1), pp.70–74.
- J. A. Cabrera, et al., 2007. Multiobjective constrained optimal synthesis of planar mechanisms using a new evolutionary algorithm. *Mechanism and Machine Theory*, 42(7), pp.791–806.
- J.A. Cabrera, A. Simon, and M. Prado, 2002. Optimal synthesis of mechanisms with genetic algorithms. *Mechanism and Machine Theory*, 37(10), pp.1165–1177.
- P.V. Chanekar and A. Ghosal, 2013. Optimal synthesis of adjustable planar four-bar crank-rocker type mechanisms for approximate multi-path generation. *Mechanism and Machine Theory*, 69, pp.263–277.
- N. Diab and A. Smaili, 2017. An Ants-Search based method for optimum synthesis of compliant mechanisms under various design criteria. *Mechanism and Machine Theory*, 114, pp.85–97. Available at: <http://dx.doi.org/10.1016/j.mechmachtheory.2017.04.004>.
- B. El-kribi, et al., 2013. Application of multi-objective genetic algorithms to the mechatronic design of a four bar system with continuous and discrete variables. 61, pp. 68–83.
- S. Erkaya and I. Uzmay, 2009. Determining link parameters using genetic algorithm in mechanisms with joint clearance. *Mechanism and Machine Theory*, 44, pp.222–234.
- G. R. Gogate and S.B. Matekar, 2012. Optimum synthesis of motion generating four-bar mechanisms using alternate error functions. *Mechanism and Machine Theory*, 54, pp.41–61.
- K. S. Hatamleh et al., 2015. Unmanned Aerial Vehicles parameter estimation using Artificial Neural Networks and Iterative Bi-Section Shooting method. *Applied Soft Computing*, 36, pp.457–467.
- R. L. Haupt and S.E. Haupt, 2003. *Practical Genetic Algorithms* 2nd ed., Hoboken, NJ, USA: John Wiley & Sons, Inc.
- J. H. Holland, 1992. Genetic Algorithms. *Scientific American*, 267, pp.66–72.
- H. K. Khalaf, 2012. *Active Control of A Piezoelectric Actuated Four-Bar Mechanism Deployed in Robotics Applications*. Jordan University of Science and Technology.
- M. Khorshidi, et al., 2011. Optimal design of four-bar mechanisms using a hybrid multi-objective GA with adaptive local search. *Mechanism and Machine Theory*, 46(10), pp.1453–1465.
- S. Krishnan and L. Saggere, 2007. A multi-fingered micromechanism for coordinated micro/nano manipulation. *Journal of Micromechanics and Microengineering*, 17, pp.576–585.
- M. A. Laribi, et al., 2004. A combined genetic algorithm-fuzzy logic method (GA-FL) in mechanisms synthesis. *Mechanism and Machine Theory*, 39, pp.717–735.
- H. C. Liaw and B. Shirinzadeh, 2009. Neural network motion tracking control of piezo-actuated flexure-based mechanisms for micro-/nanomanipulation. *IEEE/ASME Transactions on Mechatronics*, 14(5), pp.517–527.
- H. C. Liaw, B. Shirinzadeh, and J. Smith, 2008. Robust motion tracking control of piezo-driven flexure-based four-bar mechanism for micro/nano manipulation. *Mechatronics*, 18(2), pp.111–120.
- C.-J. Lin and S.-R. Yang, 2006. Precise positioning of piezo-actuated stages using hysteresis-observer based control. *Mechatronics*, 16(7), pp.417–426. Available at: <http://linkinghub.elsevier.com/retrieve/pii/S0957415806000353>.
- C. J. Lin and P. T. Lin, 2012. Particle swarm optimization based feedforward controller for a XY PZT positioning stage. *Mechatronics*, 22(5), pp.614–628.
- M. Lopez-Martinez and E. Campo, 2003. Micro-Nano Technologies for Cell Manipulation and Subcellular Monitoring. *Intechopen.Com*.

- M. Nambi, A. Damani, and J.J. Abbott, 2012. An Empirical Study of Static Loading on Piezoelectric Stick-Slip Actuators of Micromanipulators. In *Int. Symp. Experimental Robotics*.
- D. Oetomo, et al., 2006. Direct Kinematics and Analytical Solution to 3RRR Parallel Planar Mechanisms. In *2006 9th International Conference on Control, Automation, Robotics and Vision*. IEEE, pp. 1–6. Available at: <http://ieeexplore.ieee.org/document/4150263/>.
- M. Sitti, 2003. Piezoelectrically actuated four-bar mechanism with two flexible links for micromechanical flying insect thorax. *IEEE/ASME Transactions on Mechatronics*, 8(1), pp.26–36. Available at: <http://ieeexplore.ieee.org/lpdocs/epic03/wrapper.htm?arnumber=1187356> [Accessed November 26, 2014].
- K.K. Tan, 2001. Computer controlled piezo micromanipulation system for biomedical applications. *Engineering Science and Education Journal*, 10, p.249.
- H. Tari and H.-J. Su, 2011. A complex solution framework for the kinetostatic synthesis of a compliant four-bar mechanism. *Mechanism and Machine Theory*, 46(8), pp.1137–1152. Available at: <http://dx.doi.org/10.1016/j.mechmachtheory.2011.03.003>.
- B. Yi and J. Liu, 2017. *Multi-objective Optimization Design of Automated Side Loader of Arm Actuator*. X. Zhang, N. Wang, & Y. Huang, eds., Singapore: Springer Singapore. Available at: <http://link.springer.com/10.1007/978-981-10-2875-5>.
- C. Zhang, P. R.L. Norton, and T. Hammonds, 1984. Optimization of parameters for specified path generation using an atlas of coupler curves of geared five-bar linkages. *Mechanism and Machine Theory*, 19(6), pp.459–466.

9 DISCLOSURE STATEMENT

No potential conflict of interest was reported by the authors.

NOTES ON CONTRIBUTORS



Laith Sawaqed, Ph.D. is the Mechanical Engineering-Acting chairperson of Department. Dr. Sawaqed holds a Bachelor's and Master's Degrees in Mechanical Engineering - Mechatronics from Jordan University of Science and Technology in 2006, 2008, respectively. He received his Doctorate in Mechanical Engineering from University of Maryland – College Park in 2013. Dr. Sawaqed's primary area of research has focused on Artificial Intelligence, Robotics, and Control Systems.



Khaled S. Hatamleh received his B.Sc. (2002) in Mechanical Engineering from JUST, Jordan. Received his M.Sc. (2006) in Industrial Automation Engineering from Yarmouk University, Jordan, and his Ph.D. (2010) in mechanical engineering from New Mexico State University, NM, USA. Currently he is an Assistant Professor at the American University of Sharjah, and JUST. His research areas are: robotics, UAV parameter estimation, IMU, and control systems.



Mohammad Abdel Kareem Jaradat received the B.Sc. degree from Jordan University of Science & Technology, Jordan, and the M.Sc. and Ph.D. degrees in mechanical engineering from Texas A&M University, College Station, TX, USA. Currently he is an Associate Professor at the American University of Sharjah, and with Jordan University of Science & Technology. During his integrated experience several projects, prototypes and publications are conducted, specialized in the following research areas: robotics, artificial intelligent systems, mechatronics system design, sensor fusion, fault diagnostics, intelligent nano-systems, intelligent control, and embedded control systems.



Qais Khasawneh received his BSc (1999) From JUST and received his MSc (2002) and PhD (2008) from the University of Akron, USA. He has been serving as an assistant professor in the mechanical engineering department/mechatronics since 2009. His research activities involve MEMS, Nanotechnology, renewable energy, and control.